

Permeability of Noble Gases through Kapton, Butyl, Nylon, and “Silver Shield”

Steven J. Schowalter, Colin B. Connolly*, John M. Doyle

Department of Physics, Harvard University, 17 Oxford St., Cambridge, MA 02138, USA

Abstract

Noble gas permeabilities and diffusivities of Kapton, butyl, nylon, and “Silver Shield” are measured at temperatures between 22°C and 115°C. The breakthrough times and solubilities at 22°C are also determined. The relationship of the room temperature permeabilities to the noble gas atomic radii is used to estimate radon permeability for each material studied. For the noble gases tested, Kapton and Silver Shield have the lowest permeabilities and diffusivities, followed by nylon and butyl, respectively.

Key words: noble gas, permeation, diffusion, Kapton, radon

1. Introduction

2 The permeability of radon through the polyimide Kapton [1] is a key
3 factor in determining its effectiveness as a gasket or membrane material in
4 certain low radioactive background experiments, such as MiniCLEAN [2, 3].
5 Kapton is a polyimide manufactured by DuPont and has applications in
6 aerospace design, electrical insulation, automotive design, vacuum experi-
7 ments, and more [4, 5, 6]. Its utility in many applications is due to its
8 ability to retain certain desirable properties when cooled to low tempera-
9 tures, for example its pliability. This is most dramatically shown by its use
10 as a superfluid-tight seal gasket at temperatures below 2 K [7]. Also, Kap-
11 ton film is relatively inexpensive and can be easily formed, making it an
12 appealing material for other experimental applications. In the MiniCLEAN
13 experiment, Kapton is a candidate to perform a sealing function for about

*Corresponding author (e-mail: connolly@physics.harvard.edu)

14 one hundred roughly 25 cm diameter flanges at temperatures between 20-
15 300 K. This gasket must keep radon from permeating into the main vacuum
16 vessel while at room temperature.

17 Here we report measurements of noble gas permeation through Kapton
18 film and other technical materials including nylon [8], butyl [9], and “Silver
19 Shield” [10], all of which have uses as gaskets, in gloveboxes, or as shielding
20 from radon permeation. Nylon is frequently used as a bagging material to
21 prevent radon from coming in contact with detector components during ship-
22 ping or storage. Butyl is an inexpensive and resilient glove material and can
23 be used as a vacuum seal gasket. Silver Shield is a composite glove or bag-
24 ging material specifically designed for low permeability that includes layers
25 EVOH (polyvinyl alcohol), which has been shown to have low permeability
26 to radon [11].

27 **2. Background**

28 Permeation is the process through which a gas passes through a solid
29 material. The permeability K is defined as

$$Q = K \frac{A}{d} \Delta P \quad (1)$$

30 where Q is the number flow rate of a test gas through a thickness d and
31 cross-sectional area A under a pressure difference ΔP . The permeability K
32 can also be written as

$$K = Db \quad (2)$$

33 where D is the diffusivity and b is the solubility of gas in the material. The
34 solubility determines the concentration of gas dissolved in the polymer at a
35 given partial pressure; the diffusivity determines the rate at which gas flows
36 in the material.

By observing the time evolution of gas permeation after establishing a
concentration gradient, it is possible to probe diffusivity independent of sol-
ubility. The solution of the one-dimensional diffusion equation [12] for gas

diffusing across a membrane of thickness d gives the gas flow Q from the low-pressure side to be

$$Q(t) = Q_0 \left[1 + 2 \sum_{n=1}^{\infty} (-1)^n \exp \left(-(n\pi)^2 \frac{d^2}{D} t \right) \right]. \quad (3)$$

where Q_0 is the final steady state flow. Note that the dynamics of the flow are determined only by d and the diffusivity D . The time taken for a significant amount of gas to permeate through the film is called the breakthrough time or lag time. Experiments measuring permeation typically define this to be

$$t_b = \frac{d^2}{6D}. \quad (4)$$

37 The determination of D and t_b from flow measurements is discussed in detail
38 in Section 4.

39 As with permeation through other polymers, the permeation of noble
40 gases through the materials studied is expected to increase with increasing
41 temperature. The permeability and breakthrough time are expected to follow
42 the relations

$$K(T) \propto \exp(-E_K/k_B T) \quad (5)$$

$$t_b(T) \propto d^2 \exp(E_D/k_B T) \quad (6)$$

43 where E_K is the energy of permeation, and E_D is the energy of diffusion.
44 In this experiment, this temperature dependence is observed and used to
45 extrapolate room temperature (22°C) xenon permeability for Kapton. Ulti-
46 mately any temperature dependence can be exploited in order to increase or
47 decrease the rate of permeation.

48 3. Experimental

49 We measure permeation using a specific gas flow method in which a con-
50 stant high pressure of gas is placed on one side of a film and the steady-state

51 pressure of permeated gas is monitored with a calibrated Residual Gas An-
52alyzer (RGA) on the low pressure, evacuated, side of the film. Our design
53enables us to measure the permeability and diffusivity for helium, neon, ar-
54gon, krypton, and xenon through various membrane materials. Due to the
55highly radioactive nature of radon, measuring the permeation of radon in
56this manner would be too onerous. Instead we estimate the permeation rate
57of radon by extrapolating from permeation data of the stable noble gases.

58 The apparatus (shown in Figure 1) consists of three major parts: a high-
59pressure inlet chamber, a low-pressure outlet chamber, and a film holder.

60 The two chambers are constructed from stainless steel tubes and VCR
61fittings and connected to two vacuum pumps. The high-pressure chamber is
62connected to a rotary vane pump which is able to evacuate the chamber to
63pressures of 10^{-3} torr prior to filling with test gas. A simple gas handling
64system introduces up to 10^3 torr of test gas into the high-pressure chamber
65(as measured by a Baratron pressure gauge). The low-pressure chamber is
66connected to a turbomolecular pump capable of evacuating the chamber to
67 10^{-6} torr, as well as to a xenon standard leak (SL), an ionization gauge, and
68an RGA.

69 The high- and low-pressure chambers are separated by a film of the ma-
70terial under study housed in a film holder. The film holder consists of two
71custom flanges, one made of brass and one made of aluminum, and each
72makes a Viton O-ring seal to one side of the Kapton film. The film is pressed
73between the O-rings, which are held in grooves in the flanges. Each flange
74has a fitting in order to connect the film holder between the high- and low-
75pressure chambers. To minimize the chances of the film warping or rupturing
76under differential pressure (as high as 10^3 torr), a depression on the inside of
77the low-pressure flange holds a stainless steel mesh with a grid size of 2 mm
78and 40% open area, which provides mechanical support for the film. The
79cross sectional area for test gas diffusion is 83 cm^2 .

80 To manipulate the temperature of the film, heater tape and insulation
81are wrapped around the metal film holder. The temperature is monitored by
82thermocouples attached at various places on the film holder.

83 An RGA is used to measure and distinguish partial pressures of different
84gases below 10^{-4} torr in the high-vacuum chamber. Once both experimental
85chambers have been evacuated, test gas (such as argon) is introduced into the
86high-pressure chamber to establish a pressure gradient across the film. As the
87test gas begins to permeate, the RGA partial pressure rises asymptotically
88to a steady state value, P_{ss} , set by the flow of the permeating gas and by the

89 pumping speed and conductance of the pumping line.

90 4. Results and Discussion

91 The time evolution of test gas partial pressure in the low-pressure chamber
92 is analyzed to determine the permeability and the diffusivity of the test gas
93 through the material under study. An example data run for argon permeating
94 through Kapton is shown in Figure 2. At $t = 0$ argon gas is inserted into
95 the high-pressure chamber and allowed to come in contact with the Kapton
96 film. Argon diffuses through the film, causing the argon partial pressure in
97 the low-pressure chamber to rise asymptotically to a steady state value, P_{ss} .
98 The diffusivity D is determined by fitting the solution to the one-dimensional
99 diffusion equation (Equation 3) to the partial pressure data shown in Figure
100 2. To fit this model to the data, we use terms up to $n = 3$, which provides
101 less than 1% deviation from the infinite sum over the entire fitting interval.
102 The breakthrough time can then be calculated using Equation 4. The fitting
103 procedure is repeated for each experiment as the film material, film thickness,
104 test gas, inlet pressure, and temperature are varied.

105 The test gas permeation rate Q is determined by comparing the steady
106 state pressure P_{ss} to the steady state pressure P_{SL} from the calibrated flow
107 of the xenon standard leak, Q_{SL} . P_{SL} was observed to remain unchanged
108 for total pressures in the low-pressure chamber below 10^{-5} torr. Q_{SL} can
109 be expressed as $Q_{SL} = P_{SL}S_{\text{eff}}^{Xe}$, where S_{eff}^{Xe} is the effective volumetric flow
110 of xenon gas from the RGA to the pump. Similarly, the flow rate of the
111 permeating test gas can be written $Q_{gas} = P_{ss}S_{\text{eff}}^{gas} = P_{ss}S_{\text{eff}}^{Xe}\sqrt{m_{Xe}/m_{gas}}$,
112 where the latter equality has used the linear dependence of volumetric flow
113 on particle velocity in the molecular flow regime. Using Equation 1 we find
114 that the permeability is given by

$$K = P_{ss} \frac{Q_{SL}}{P_{SL}} \sqrt{\frac{m_{Xe}}{m_{gas}}} \frac{d}{A\Delta P}. \quad (7)$$

115 We can then use Equation 2 to calculate the solubility b from K and D .

116 In order to check for systematic error, we varied several features of our
117 experiment. To ensure that the test gas did not saturate the film material,
118 we varied the inlet pressure of helium and neon and found that inlet pressure

119 had no effect on K (shown in Figure 3), implying that the film is not satu-
120 rated over the test gas pressure range. We also tested the diffusive model of
121 permeation by measuring K and D for neon permeating 2 and 5 mil thick
122 Kapton films. K was unchanged by varying film thickness and t_b increased
123 by a factor of $6.2 \pm .5$, consistent with the factor of 6.25 predicted by the
124 model for a constant D . Lastly, we ensured K and D were not affected by
125 varying the mesh size. Similar tests were repeated for each material studied.

126 As previously mentioned, the permeation rate can be manipulated by
127 varying the temperature of the material. Increasing the film temperature
128 increases permeation rate, increasing K and D and decreasing t_b . By mea-
129 suring K and D at high temperatures, we can extrapolate room temperature
130 data. Due to the properties of the materials, Kapton is the only material
131 through which permeation at elevated temperatures were measured.

132 Using methods described above, we determined the permeability and dif-
133 fusivity of argon, krypton, and xenon through 2 and 5 mil Kapton films at
134 various temperatures. These results are shown in Figures 4 and 5. For con-
135 venience, the diffusivities have been converted in Figure 5 to breakthrough
136 times through a 2 mil film using Equation 4. As expected, we observe an
137 increase in K and D and thus a decrease in t_b for each gas with increasing
138 film temperature. The Kapton film is not noticeably affected otherwise by
139 the elevated temperatures, which are far below the melting point.

140 Measuring the permeability of xenon through Kapton at room tempera-
141 ture would take many days. Instead, the data in Figure 4 is fit to Equation 5
142 and we extrapolate the 22°C permeability of xenon through Kapton. Room
143 temperature breakthrough time of xenon through Kapton is not extrapolated
144 due to insufficient t_b data at high temperatures.

145 Using the methods discussed in the previous sections, we are able to
146 determine the stable noble gas permeability, diffusivity, and solubility of the
147 four materials studied at 22°C. This data is shown in Table 1.

148 5. Model for Noble Gas Permeability of Polymers

149 The permeation of some polymers has been observed to show an expo-
150 nential dependence with the square of the atomic radius of the permeating
151 gas [13]. The noble gas permeabilities and breakthrough times of the four
152 materials studied are plotted in this manner in Figures 6 and 7 along with
153 exponential fits for each material. The atomic radii, taken from [14], are the
154 same as those used in [13].

155 The room temperature permeation of xenon through Silver Shield is not
156 measured due to the length of time required for the measurement. Silver
157 Shield material cannot be heated to temperatures above 50°C, thus we cannot
158 decrease the experimental time and extrapolate room temperature values in
159 the manner described above. Room temperature diffusivity of xenon through
160 Kapton is also not included due to insufficient data for extrapolation.

161 Using the empirical model described above, we estimate K and t_b for
162 radon permeation through Kapton, butyl, nylon, and Silver Shield at 22°C.
163 These estimates are shown in Table 2. Both K and t_b are typically monotonic
164 with respect to the square of the atomic diameter of the permeating gas. Thus
165 the measured values for xenon can be taken as a conservative upper and lower
166 bound for the radon values for K and t_b respectively. These bounds are also
167 included in Table 2. Krypton bounds are used for materials whose xenon
168 permeation values were not measured.

169 The uncertainty of the radon permeation estimates is dominated by sys-
170 tematic uncertainty in applying the model function. Although the fits of
171 permeability to this function in Figure 6 agree with the data rather well over
172 several orders of magnitude of permeability, and similar fits in [13] provided
173 realistic estimates of radon permeability, there is considerable uncertainty
174 in the extrapolations to radon. For example, the fit underestimates helium
175 permeability and overestimates neon permeability for all materials studied,
176 suggestive of a more complex functional form. Similarly, the fits of break-
177 through times to the same model in Figure 7 assume a similar or weak de-
178 pendence of solubility on the square of the atomic diameter, which may not
179 be the case. With the limitations of the model in mind, the bounds given by
180 xenon or krypton measurements reflect the estimation uncertainty.

181 The radon isotope of concern to low radioactive background experiments
182 is radon-222, which has a half-life of 3.8 days (3.3×10^5 s) [15]. A gasket
183 suitably impermeable to radon for these experiments should have a break-
184 through time that is long compared to the radon-222 half-life. Since $t_b \propto d^2$,
185 t_b can be greatly increased by increasing the distance over which gas per-
186 meates. If t_b is much longer than the radon-222 half-life, then only a small
187 fraction of radon atoms will permeate a gasket before decaying. Addition-
188 ally, the radon exposure time can be minimized to reduce the total number
189 of dissolved radon atoms.

190 6. Conclusion

191 We use a gas-flow method to measure and calculate previously unrecorded
192 data for noble gas permeability, diffusivity, and solubility of Kapton, butyl,
193 nylon, and Silver Shield at 22°C. We note that these properties can vary on
194 the details of manufacture and especially between different manufacturers.
195 The temperature dependence of permeation can be exploited to manipulate
196 the permeation rate, as demonstrated here. The permeability of Kapton is
197 measured at higher temperatures up to 120°C using argon, krypton, and
198 xenon, and these values are used to extrapolate the xenon permeability of
199 Kapton at 22°C. Based on the empirical model used previously in [13], we
200 estimate radon permeability and breakthrough time of 2 mil films at 22°C.
201 With this information, the suitability of the use of the materials studied as
202 gasket or glove materials in low background radiation experiments can be
203 appropriately determined.

204 7. Acknowledgments

205 We would like to thank the DEAP/CLEAN collaboration for helpful dis-
206 cussions, and the Weak Interactions team at Los Alamos National Labora-
207 tory for the suggestion of testing Silver Shield and for providing the nylon
208 material.

209 References

- 210 [1] *Kapton Polyimide Film: General Specifications*. DuPont, 1007 Market
211 Street, Wilmington, DE 19898.
- 212 [2] D. N. McKinsey and K. J. Coakley. Neutrino detection with CLEAN.
213 *Astropart. Phys.*, 22:355–368, 2005.
- 214 [3] D. N. McKinsey. The Mini-CLEAN experiment. *Nuc. Phys. B*, 173:
215 152–155, 2007.
- 216 [4] A. N. Hammoud, E. D. Baumann, E. Overton, I. T. Myers, J. L. Suthar,
217 W. Khachen, and J. R. Laghari. High temperature dielectric proper-
218 ties of Apical, Kapton, Peek, Teflon AF, and Upilex polymers. *NASA*
219 *STI/Recon Technical Report N*, 92:28675, June 1992.

- 220 [5] Tatsumi Hioki, Shoji Noda, Masahiro Sugiura, Mitsutaka Kakeno,
221 Kenichi Yamada, and Junichi Kawamoto. Electrical and optical prop-
222 erties of ion-irradiated organic polymer kapton h. *Appl. Phys. Lett.*, 43
223 (1):30–32, 1983.
- 224 [6] B. Baudouy. Kapitza resistance and thermal conductivity of Kapton in
225 superfluid helium. *Cryog.*, 43(12):667 – 672, 2003.
- 226 [7] R. C. Richardson and E. N. Smith. *Experimental Techniques in Con-*
227 *densed Matter Physics at Low Temperatures*. Addison-Wesley, 1988.
- 228 [8] *Nylon Film Properties*. KNF Corporation, 734 West Penn Pike,
229 Tamaqua, PA. 18252.
- 230 [9] Butyl glove, rough finish, 16-mil thickness, 11”, North Safety Products,
231 2000 Plainfield Pike, Cranston, RI 02921.
- 232 [10] *Silver Shield/4H Gloves and Accesories*. North Safety Products, 2000
233 Plainfield Pike Cranston, RI 02921, 2001.
- 234 [11] Ludwig De Braeckleer. neutrino physics with the KamLAND detector.
235 *Nuclear Physics B (Proc. Suppl.)*, 87:312–314, 2000.
- 236 [12] Richard M. Barrer. *Diffusion In and Through Solids*. Cambridge Uni-
237 versity Press, 1941.
- 238 [13] H. George Hammon, Klaus Ernst, and John C. Newton. Noble gas
239 permeability of polymer films and coatings. *J. Appl. Polym. Sci.*, 21:
240 1989–1997, 1977.
- 241 [14] J. O. Hirschfelder, C. F. Curtiss, and R. B. Bird. *Molecular Theory of*
242 *Gases and Liquids*. Wiley, 1964.
- 243 [15] T. V. Ramachandran, B. Y. Lalit, and U. C. Mishra. Measurement
244 of radon permeability through some membranes. *Radiat. Meas.*, 13(1):
245 81–84, 1987.

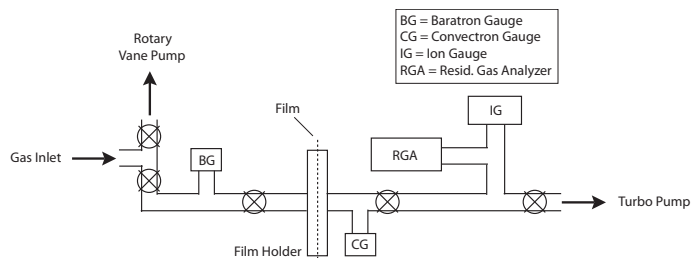


Figure 1: A schematic of the apparatus used to measure permeation.

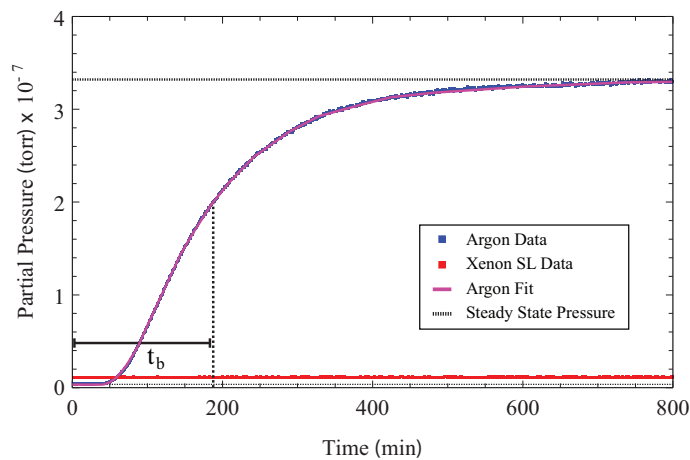


Figure 2: (Color online) Sample data used to determine permeability and diffusivity. At $t = 0$, gas is introduced to the high-pressure chamber and allowed to come in contact with the film. Due to the pressure difference across the film, the gas begins to permeate the film. The argon gas partial pressure rises asymptotically to a steady state pressure after a characteristic breakthrough time, t_b , defined in Equation 4.

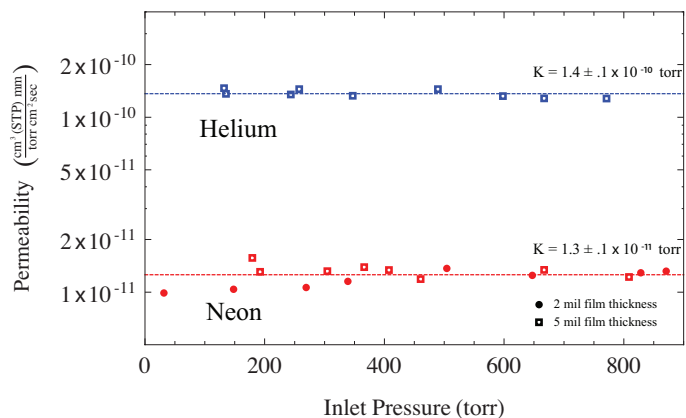


Figure 3: (Color online) The permeability of Kapton is independent of film thickness and inlet pressure, as shown with He and Ne.

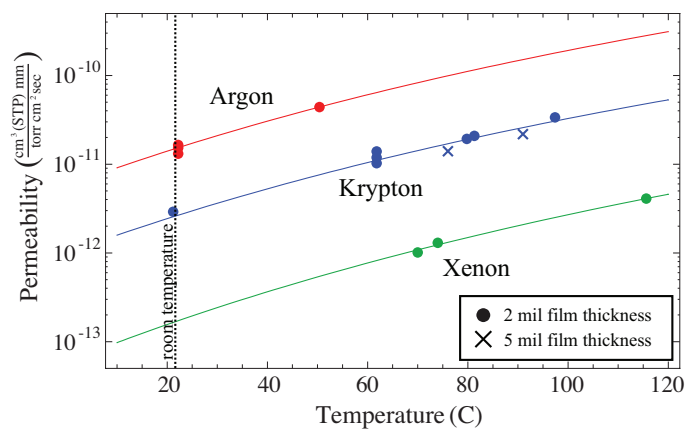


Figure 4: (Color online) The temperature dependence of Ar, Kr, and Xe permeability through Kapton. The curves are fits to Equation 5. The Xe fit is used to extrapolate the 22°C xenon permeability.

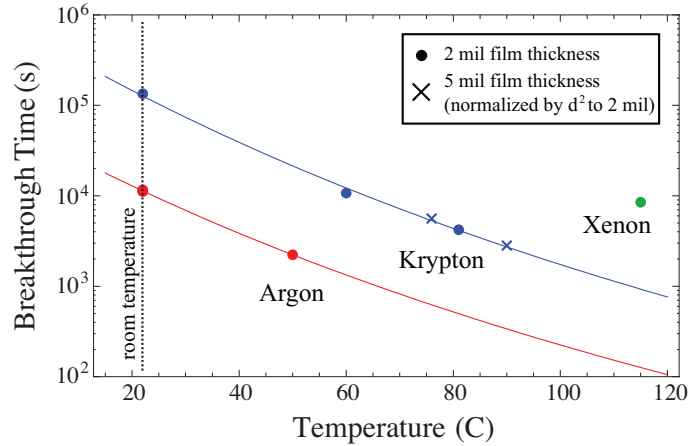


Figure 5: (Color online) The temperature dependence of the breakthrough time of Ar and Kr permeating Kapton. The data using 5 mil film thickness is scaled to 2 mil values for comparison using Equation 4. The curves are fits to Equation 6.

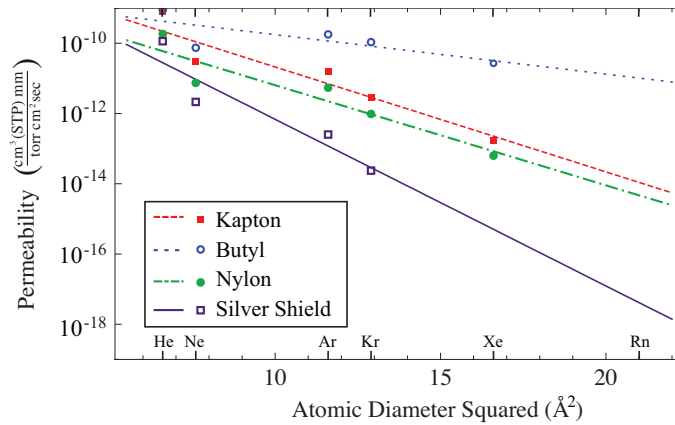


Figure 6: (Color online) The exponential trend of room temperature (22°C) permeabilities versus the square of the atomic diameter of the permeating gas. Xenon permeation was not measured using Silver Shield.

| Material | Gas | $K(\frac{\text{cm}^3 \text{ at STP mm}}{\text{s torr cm}^2})$ | $D(\frac{\text{cm}^2}{\text{s}})$ | t_b (s) | $b(\frac{\text{cm}^3 \text{ at STP}}{\text{torr cm}^3})$ |
|----------------------|-----|---|-----------------------------------|-------------------|--|
| Kapton | He | 8.0×10^{-10} | 1.2×10^{-6} | 3.7 | 5.5×10^{-4} |
| | Ne | 3.1×10^{-11} | 9.0×10^{-8} | 48 | 3.4×10^{-5} |
| | Ar | 1.5×10^{-11} | 3.8×10^{-10} | 1.1×10^4 | 3.9×10^{-3} |
| | Kr | 2.9×10^{-12} | 3.2×10^{-11} | 1.3×10^5 | 9.0×10^{-3} |
| | Xe | $1.7 \times 10^{-13} \dagger$ | | | |
| Butyl | He | 1.0×10^{-9} | 9.5×10^{-7} | 4.5 | 1.1×10^{-4} |
| | Ne | 7.4×10^{-11} | 2.0×10^{-7} | 22 | 3.8×10^{-5} |
| | Ar | 1.8×10^{-10} | 1.9×10^{-8} | 2.3×10^2 | 9.7×10^{-4} |
| | Kr | 1.1×10^{-10} | 5.5×10^{-9} | 7.9×10^2 | 2.0×10^{-3} |
| | Xe | 2.7×10^{-11} | 3.7×10^{-9} | 1.2×10^3 | 7.3×10^{-4} |
| Nylon | He | 1.8×10^{-10} | 7.3×10^{-7} | 5.9 | 2.5×10^{-5} |
| | Ne | 7.4×10^{-12} | 9.2×10^{-8} | 47 | 8.0×10^{-6} |
| | Ar | 5.4×10^{-12} | 1.0×10^{-9} | 4.3×10^3 | 5.4×10^{-4} |
| | Kr | 9.7×10^{-13} | 1.2×10^{-10} | 3.5×10^4 | 7.9×10^{-4} |
| | Xe | 6.3×10^{-14} | 7.4×10^{-12} | 5.8×10^5 | 8.5×10^{-4} |
| Silver Shield | He | 6.9×10^{-10} | 1.9×10^{-6} | 2.2 | 3.6×10^{-5} |
| | Ne | 2.1×10^{-12} | 1.4×10^{-7} | 30 | 1.5×10^{-6} |
| | Ar | 2.5×10^{-13} | 4.2×10^{-10} | 1.0×10^4 | 6.0×10^{-5} |
| | Kr | 2.3×10^{-14} | 3.1×10^{-11} | 1.4×10^5 | 7.5×10^{-5} |
| Relative Uncertainty | | 50% | 10% | 10% | 50% |

Table 1: Summary of room temperature permeation information for He, Ne, Ar, Kr, and Xe through Kapton, butyl, nylon, and Silver Shield. For convenient comparison, t_b is calculated from Equation 4 for 2 mil material thickness. Uncertainty in K and b is based upon the systematic error in calibrating test gas flow with the xenon standard leak. Uncertainty in D and t_b is dominated by the uncertainty in determining film thickness. The value of K for xenon permeating Kapton marked with a \dagger has been extrapolated from higher temperature data using Equation 5.

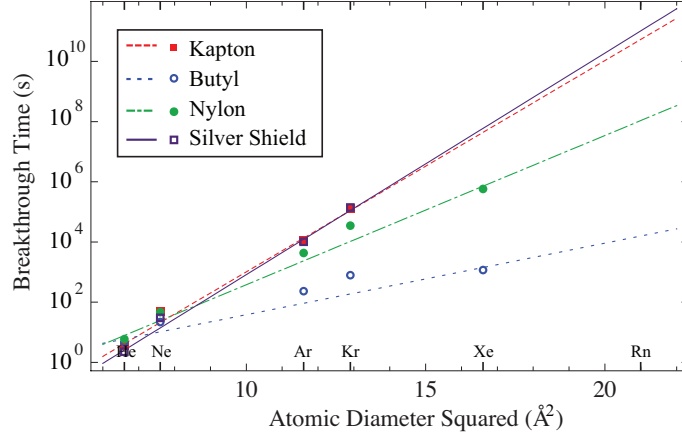


Figure 7: (Color online) The exponential trend of room temperature (22°C) breakthrough times versus the square of the atomic diameter of the permeating gas. The data are scaled to 2 mil thickness for comparison using Equation 4. Xenon breakthrough time was not determined for Kapton or Silver Shield.

| Material | Value | Rn Estimation | Xe Bound |
|---------------|-------|---------------------|--|
| Kapton | K | 1×10^{-14} | $1.7 \pm 0.8 \times 10^{-13}$ |
| | t_b | 5×10^{10} | $1.3 \pm 0.1 \times 10^5$ (Kr Bound) |
| Butyl | K | 1×10^{-11} | $2.7 \pm 1.4 \times 10^{-11}$ |
| | t_b | 2×10^4 | $1.2 \pm 0.1 \times 10^3$ |
| Nylon | K | 5×10^{-15} | $6.3 \pm 3.2 \times 10^{-14}$ |
| | t_b | 1×10^8 | $5.8 \pm 0.6 \times 10^5$ |
| Silver Shield | K | 4×10^{-18} | $2.3 \pm 1.2 \times 10^{-14}$ (Kr Bound) |
| | t_b | 1×10^{11} | $1.4 \pm 0.1 \times 10^5$ (Kr Bound) |

Table 2: Summary of estimations and bounds for room temperature Rn K and t_b through 2 mil material. The uncertainties for the Xe and Kr bounds are the same as in Table 1. The Xe and Kr bounds reflect the systematic uncertainty of the model used to estimate the Rn values.